

Received November 9, 2020, accepted November 23, 2020, date of publication November 30, 2020, date of current version December 16, 2020.

Digital Object Identifier 10.1109/ACCESS.2020.3041359

Effects of Silicone Oil on Stiffness and Damping of Rubber-Silicone Oil Combined Damper for Reducing Shaft Vibration

MIAOMIAO LI¹, JINGYU ZHANG¹, CHUANGUO WU¹, RUPENG ZHU¹, WEIFANG CHEN¹, CHENG DUAN², AND XIONG LU²

¹National Key Laboratory of Science and Technology on Helicopter Transmission, Nanjing University of Aeronautics and Astronautics, Nanjing 210016, China

²AECC Hunan Aviation Powerplant Research Institute, Zhuzhou 412000, China

Corresponding author: Miaomiao Li (limiaomiao@nuaa.edu.cn)

This work was supported in part by the National Natural Science Foundation of China under Grant 51775265, and in part by the National Key Laboratory of Science and Technology on Helicopter Transmission, Nanjing University of Aeronautics and Astronautics, under Grant HTL-A-19G09.

ABSTRACT The helicopter tail drive shaft system is a typical multi-point supported drive shaft system, with a long span that can lead to serious vibration problems. Shaft vibration can be effectively reduced by installing a rubber-silicone oil combined damper between the bearing and bearing pedestal at the support point along the tail drive shaft. Stiffness and damping characteristics of the rubber-silicone oil combined damper are important factors affecting shaft vibration. In this study, the effects of silicone oil on the stiffness and damping of rubber-silicone oil combined damper were analyzed through simulations. The simulation method was experimentally verified and factors influencing the static stiffness, dynamic stiffness, and damping characteristics of the damper were investigated. In addition, the influence of damper dimensions and external excitation frequency on the stiffness and loss factor of the damping ring in the presence and absence of silicone oil were examined. The presence of silicone oil increases the difference between the dynamic stiffness and the loss factor. As the viscosity of the silicone oil increases, the static stiffness, dynamic stiffness, and loss factor of rubber-silicone oil combined dampers increase. The results have important guiding significance in the design of dampers for shafting systems.

INDEX TERMS Rubber-silicone oil combined damper, stiffness, damping, silicone oil.

I. INTRODUCTION

Dynamic characteristics of the helicopter tail drive shaft have a critical influence on the overall performance of the helicopter. The long span of the helicopter tail drive shaft system is a typical multi-support shaft system. The shaft sections are connected by flexible couplings, which can introduce serious vibration problems. Therefore, damping elements are often used to effectively reduce vibrations in the tail drive shaft system.

Rubber dampers are widely used in automobiles, ships, motor cars, etc. to achieve a wide range of vibration damping effects [1]–[3], which depend on the shape of the damper, material, and structure of the mold [4]. A large body of research has been carried out on the damping effects of

rubber dampers. Lee and Youn [5] proposed a topology optimization method for the design of rubber isolators considering both static and dynamic mechanical behaviors of rubber. Guo *et al.* [6] established a dynamic model of a rubber isolator by superimposing hyperelastic, viscoelastic, and elastoplastic models, and predicted the correlation between the vibration isolator amplitude and frequency. Yu *et al.* [7] used a combination of tests and simulations to study the dynamic stiffness and damping characteristics of silicone rubber isolators and showed that dynamic stiffness and damping characteristics of the isolators are non-linear and obtained the displacement transfer rates. Zhu and Youxiang [8] prepared a silicone rubber composite dielectric elastomer and studied its properties. Ziqi *et al.* [9] investigated the stress-strain hysteresis behavior of silicone rubber-based electrorheological elastomers under different electric field strengths, shear frequencies, and strain amplitudes. In addition, dynamic

The associate editor coordinating the review of this manuscript and approving it for publication was Hassen Ouakad ¹.

viscoelasticity of the elastomers was analyzed under various operating conditions. The results were then used to modify the nonlinear constitutive models and parameter identification was performed. Wang *et al.* [10] studied the dynamic performance of rubber components under compressive and shear stresses, introduced a nonlinear dynamic model of a rubber damper in a track fixation, and analyzed the dynamic stiffness and damping of the damper. Jingzhi *et al.* [11] performed dynamic tests on rail fastener rubber parts under various working conditions and obtained dynamic force-displacement curves. Dynamic characteristics of the rubber parts were evaluated and the amplitude- and frequency-dependent behavior of parts with different rubber compositions were analyzed. Quanshan *et al.* [12] proposed a uniaxial compression test equivalent to the axial tensile rubber constitutive test method and combined the test data and theory to establish a rubber constitutive model; then the finite element method was used to analyze static deformation of the rubber damper in a marine environment. Numerical results and test data were compared, which shows that the second-order polynomial constitutive model describe the deformation of the superelastic rubber damper commendably. Gang *et al.* [13] conducted an in-depth analysis of the rubber bushings characteristics of an automobile suspension and identified and fitted superelastic coefficients of the constitutive model using finite element software. Abdulla *et al.* [14] derived the relationship between the linear displacement and angular displacement of a natural rubber engine vibration isolator. Liming *et al.* [15] performed a finite element analysis of neck-type vibration damping pads made of different rubber materials, such as silicone rubber, natural rubber, butyl rubber, foam rubber materials and simulated vibration damping pad failure. The failure location provides a reasonable basis for damping pads design of high-speed machine tools. Keqi *et al.* [16] performed dynamic impact tests on a rubber damper for railway tracks and established a dynamic model, as well as two different kinds of mass models for simulating the impact mass. Results of the finite element analysis were consistent with experimental data suggesting the model can accurately simulate the dynamic response of the rubber vibration reduction system, which could shorten the design and optimization process.

The vibration damping effects of rubber dampers made of different raw materials will vary. Since the elastic hysteresis is typically small and rubber materials do not provide appropriate damping in wide frequency ranges. To improve damping properties, silicone oil is often used alongside the damping components as a damping fluid. The combined viscoelastic damping characteristics of the rubber material and high viscous friction damping characteristics of the silicone oil can effectively reduce vibration. The rubber-silicone oil combined damper was first used in the S-64 helicopter of the US Sikorsky company in 1962 [17]. The damper consists of a tightly vulcanized ring structure with an outer hollow rubber ring and inner metal bushing and the cavity of the hollow rubber ring is filled with silicone oil. Xilong [18]

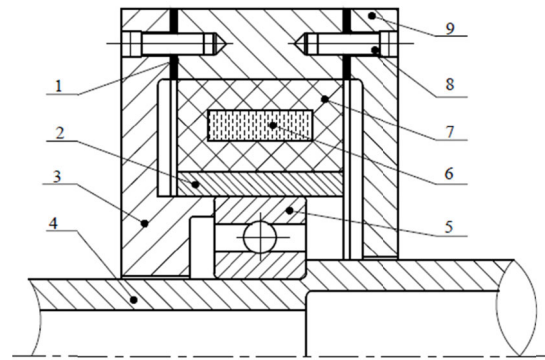


FIGURE 1. Schematic diagram of installation of rubber-silicone oil combined damper 1- elastic washer; 2- metal bush; 3- left end cover; 4- hollow shaft; 5- bearing; 6-silicone oil; 7-hollow rubber ring; 8-screw; 9-right end cover.

introduced a mathematical model of the radial stiffness and damping effects of an annular rubber silicone oil damper and analyzed the influence of rubber size on the radial stiffness of the damper. The effects of silicone oil on the damping of the rubber-silicone oil combination damping ring were also effectively analyzed, however, validation tests were not performed to verify the simulation results. Weiming [19] analyzed the effect of the number preload cycles on the uniaxial tensile properties of rubber pieces. He studied the static and dynamic characteristics of solid rubber rings and rubber silicone oil rings, the rubber silicone oil ring he studied has two metal oil nozzles. The rigidity of the metal oil nozzles is much greater than that of the rubber. It is not easy to determine the effect of the presence of metal on rubber stiffness and damping.

To date, abundant research has been carried out on the vibration damping of silicone oil, whereas studies on the influence of silicone oil on the rubber-silicone oil combined damper are currently lacking. This paper presents a three-dimensional model of a rubber-silicone oil combined damper. A combination of tests and simulations were used to analyze the influence of the presence or absence of silicone oil and viscosity of the oil on the static stiffness, dynamic stiffness, and loss factor of the damper.

II. ESTABLISHMENT OF RUBBER-SILICONE OIL COMBINED DAMPER MODEL

The rubber-silicone oil combined damper is typically installed on the helicopter tail drive shaft for radial vibration damping of the shaft system. A schematic diagram of the damper installation is shown in Figure 1. The rubber-silicone oil combined damper and the metal ring are bonded as a whole using certain vulcanization process. The outer ring surface of the rubber silicone oil damping ring is connected with the bearing housing hole through an interference fit, and the inner surface of the metal ring is connected with the bearing through an interference fit. The bearing is sleeved on the shaft through an interference fit. Vibrations are transmitted from the shaft to the rubber silicone oil damping ring via the bearing.

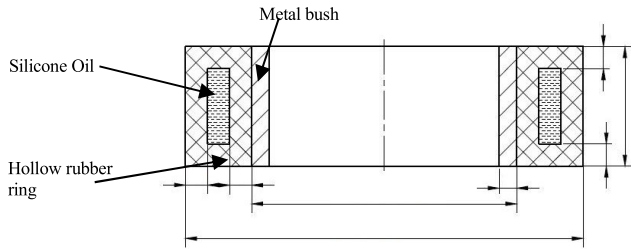


FIGURE 2. Drawing of rubber-silicone oil combined damper.

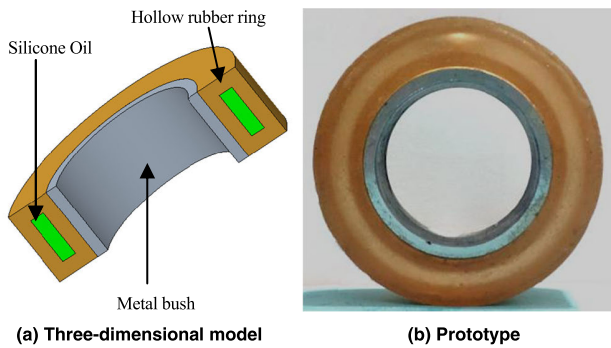


FIGURE 3. Model of rubber-silicone oil combined damper.

To study the effects of silicone oil on the stiffness and damping characteristics of rubber-silicone oil combined dampers with different structural parameters under various operating conditions, reference dimensions of the parameterized rubber-silicone oil combined dampers were established, as shown in Figure 2: The hollow rubber ring wall thickness t is 5 mm; the height of the rubber-silicone oil combined damper h is 27 mm; the inner diameter of the hollow rubber ring $2 \times r_{inner}$ is 60 mm; the outer diameter of the hollow rubber ring $2 \times r_{exterior}$ is 90 mm.

For assembly of the hollow rubber ring and the metal bush, the height of the metal bush should be consistent with its height, the outer diameter of the metal bush is consistent with the inner diameter, and the thickness of the metal bush is 4 mm. Then, considering the silicone oil and hollow rubber ring assembly, the thickness of the silicone oil is set to $(ds_r_{exterior} - ds_r_{inner} - 4 \times ds_r_{thick})/2$ mm, the reference value is 5 mm; the height of the silicone oil is $(ds_{height} - 2 \times ds_r_{thick})$ mm, the reference value is 17 mm. A drawing of the three-dimensional model of the rubber-silicone oil combined damper based on the reference value is presented in Figure 3(a) and the prototype is shown in Figure 3(b).

The manufactured rubber-silicone oil combined damper will be installed on the rotor test bench to study the vibration damping effect of rubber-silicone oil combined damper with different stiffness and damping parameter. The rotor test bench equipped with rubber-silicone oil combined damper is shown in Figure 4, and its speed range is 0-1000rpm. The vibration of the shaft is the excitation source of the rubber-silicone oil combined damper.

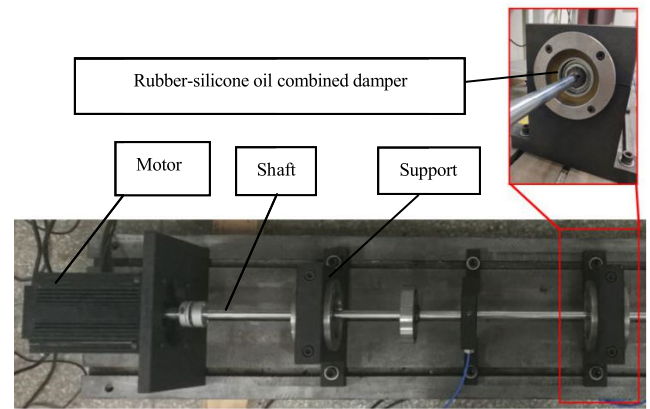


FIGURE 4. Rotor test bench with rubber-silicone oil combined damper.

III. EFFECT OF SILICONE OIL ON STATIC STIFFNESS OF COMBINED DAMPER

A. SIMULATION AND EXPERIMENTAL VERIFICATION OF STATIC STIFFNESS CHARACTERISTICS OF COMBINED DAMPER

The rubber-silicone oil combined damper contains a hollow rubber ring and silicone oil. During the working process, the silicone oil interacts with the rubber and deformation of the rubber causes the silicone oil to deform and move. In a similar way, deformation of the silicone oil will exert a force on the rubber.

To simulate the working conditions of the rubber-silicone oil combined damper, it is necessary to use both the fluid module and solid module in finite element software to perform a fluid-structure coupling simulation. The density of mental bush is 7850 kg/m^3 , the Poisson's ratio is 0.3, and elastic modulus of $2 \times 10^{11} \text{ Pa}$ was selected.

It is necessary to define the rubber material using the hyperelastic constitutive and the viscoelastic constitutive. The superelastic constitutive model is the Neo-Hookean model. The viscoelastic constitutive model is the generalized Maxwell model represented by a third-order Prony series.

The Neo-Hookean model is a constant shear model, which can only be used to predict the mechanical behavior of uniaxial tensile rubber with strain ranges between 30% and 40%, and pure shear rubber with strain ranges between 80% and 90%. The model is the simplest form of elastic body strain energy function, and can be expressed as follows:

$$W = C_{10}(I_1 - 3) \quad (1)$$

where I_1 is the first-order strain invariant, $C_{10} = 0.5 \mu_G$, and μ_G is the material shear modulus.

The generalized Maxwell model includes the expressions for both the energy storage and loss modulus of Prony series:

$$E'(\omega) = E_0 \left[1 - \sum_{i=1}^n \alpha_i^G \right] + E_0 \sum_{i=1}^n \left(\frac{\alpha_i^G \omega^2 (\tau_i^G)^2}{1 + \omega^2 (\tau_i^G)^2} \right) \quad (2)$$

TABLE 1. Prony coefficients.

Shear relative modulus	Value	Relaxation time	Value
α_1^G	0.10282707	τ_1^G	0.029022948
α_2^G	0.57009933	τ_2^G	0.00081871047
α_3^G	0.05473521	τ_3^G	0.7853139

$$E''(\omega) = \sum_{i=1}^n E_i \frac{\omega \tau_i^G}{1 + \omega^2(\tau_i^G)^2} = E_0 \sum_{i=1}^n \left(\frac{\alpha_i^G \omega \tau_i^G}{1 + \omega^2(\tau_i^G)^2} \right) \quad (3)$$

In Equation (3), E_0 is the instantaneous modulus; g_i is the ratio between the spring elastic modulus and the total elastic modulus in i -th Maxwell model; τ_i is the relaxation time of the i th Maxwell model.

The Curve Fitting module in finite element software contains commonly used hyperelastic constitutive models. The stress-strain curve of the material can be obtained through the mechanical performance test of the material [19]. The stress-strain data obtained from the test can be imported into this module. The required constitutive model parameters will be automatically fitted by finite element software. The hyperelastic constitutive parameters can be obtained by fitting the experimental data and the parameter C_{10} is equal to 3.2487×10^6 . The parameters of the viscoelastic constitutive model are shown in Table 1.

To simulate the working conditions of the rubber-silicone oil combined damper, fluid-structure coupling simulations were performed using finite element software. The Transient module is used to analyze the solid part, and the fluent module is used to calculate the fluid part. The two-way fluid-solid coupling calculation is carried out through the coupling module to calculate the static and dynamic stiffness of the rubber-silicone oil combined damper. Before performing simulations, the fluid domain and solid domain of the rubber-silicone oil combined damper were pre-processed separately and boundary conditions were set. First, the fluid domain was set up. The viscosity of the fluid (silicone oil) was set to 0.096 kg/(m·s). The fluid domain mesh of the rubber-silicone oil combined damper is illustrated in Figure 5(a). The number of nodes in the fluid domain mesh is 4720 and the number of cells is 3186. The hollow rubber ring of the corresponding solid domain and the entire inner ring surface of the hollow cavity of the hollow rubber ring were selected as the fluid-solid coupling surface, which also corresponds to the fluid-solid coupling surface of the silicone oil in the fluid domain. The solid domain mesh of the rubber-silicone oil combined damper is presented in Figure 5(b). The number of nodes in the solid domain mesh is 78862, and the number of elements is 15449.

From Figure 1, it can be seen that the outer ring of the rubber-silicone oil combined damper is flush with the base; therefore, the outer ring surface of the rubber-silicone oil combined damper was set as a fixed constraint. Considering the inner ring surface of the hollow rubber ring and

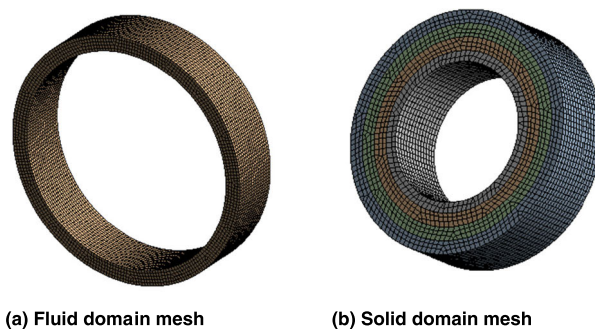


FIGURE 5. Mesh generation of rubber-silicone oil combined damper.

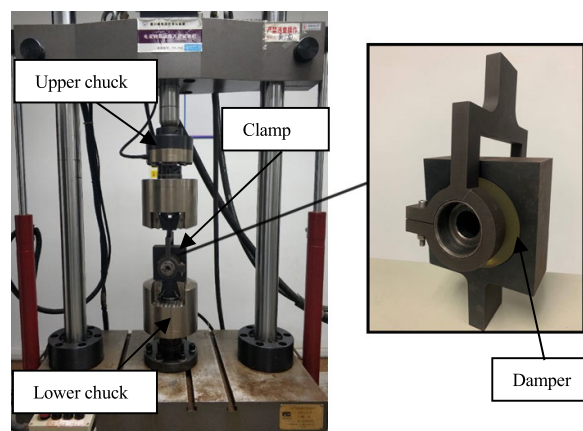


FIGURE 6. Static tensile testing of rubber-silicone oil combined damper.

the outer ring surface of the metal bush are integrated by vulcanization and bonding, the interface between the rubber and metal surfaces was set as a restricted bonded in our simulations. A static analysis was performed to determine the relationship between the load and deformation of the rubber-silicone oil combined damper. According to Standard GB/T15168-2013[20], static stiffness can be calculated as

$$K_s = \frac{\Delta F}{\Delta X} \quad (4)$$

where ΔF is the increase in static load, N; ΔX is the increase in static deformation, mm.

To verify the simulation results, static tensile tests of the rubber-silicone oil combined damper were performed using the PA-100 electro-hydraulic servo dynamic and static universal testing machine. It's maximum dynamic working force is 80KN, its maximum working frequency is 10Hz, and its maximum working displacement is 100mm. Before the test, the rubber silicone oil combined damper was installed on the clamp, and the clamp was then tightened using the upper and lower chucks of the PA-100 machine. During the testing, the lower chuck remained fixed, while the upper chuck moved in an up-and-down cycle, which was used to drive the damping via the clamp, as shown in Figure 6. The relationship between the load and deformation of the rubber-silicone combined damper is shown in Figure 7.

The simulation and test results in Figure 7 illustrates that in the elastic deformation range of 0.5 mm, the relationship

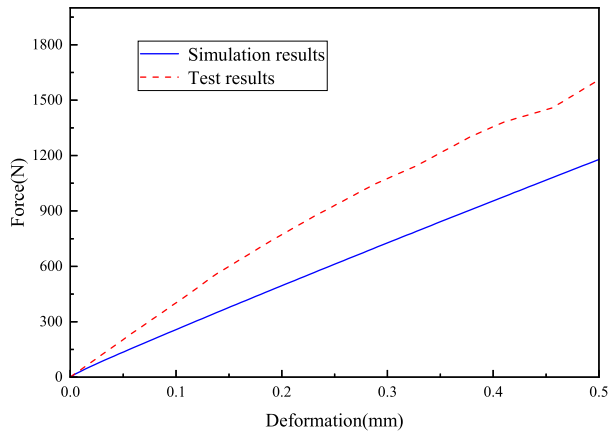


FIGURE 7. Static load-deformation curve of rubber-silicone oil combined damper.

TABLE 2. Comparison of static stiffness values obtained through simulations and static testing of combined damper.

Simulation static stiffness	Test static stiffness	Error
$2.331 \times 10^6 \text{ N/m}$	$2.558 \times 10^6 \text{ N/m}$	8.9%

between load and deformation of the rubber-silicone oil combined damper is approximately linear under static loading; therefore, the load-deformation curve can be used to solve the static stiffness of the rubber-silicone oil combined damper within this range. It can be seen from Figure 7 that the slope of the test data curve is greater than the slope of the simulation data curve, so the stiffness obtained from the test result is greater than the stiffness obtained using the simulation. According to equation (4), the static stiffness of the rubber-silicone oil combined damper is $2.331 \times 10^6 \text{ N/m}$, the test static stiffness of the rubber-silicone oil combined damper is $2.558 \times 10^6 \text{ N/m}$. A comparison of the static test and simulation results is presented in Table 2. The error of 8.9% demonstrates that the simulation results is accurate. Differences among simulation and test results are mainly owing to the stiffness of metal clamp, which is greater than the stiffness of the rubber silicone oil combined damper, resulting in a higher measured stiffness values compared to the simulations.

B. ANALYSIS OF THE EFFECT OF SILICONE OIL ON STATIC STIFFNESS OF COMBINED DAMPER

1) THE STATIC STIFFNESS CHARACTERISTICS OF DAMPER IN THE PRESENCE OR ABSENCE OF SILICONE OIL

The static stiffness of the rubber-silicon oil combined damper will be affected by the outer diameter, inner diameter, wall thickness, and height of the hollow rubber ring. In the present paper, the effect of the presence or absence of silicone oil on the static stiffness of rubber-silicone oil combined dampers were analyzed while varying with four different structural parameters. The viscosity of the silicone oil is 0.096 kg/(m·s) and the reference values are: outer diameter is 90 mm, inner diameter is 60 mm, height is 27 mm, and wall thickness is 5 mm. The parameters were varied, as follows: outer diameter

TABLE 3. Properties of silicone oil with different viscosities.

Silicone oil grade	Viscosity (kg/(m·s))	Density (kg/m ³)
100cSt	0.096	960
1000cSt	0.971	971
5000cSt	4.86	972
12500cSt	12.175	974

of 82 mm, 86 mm, 90 mm, 94 mm, and 98 mm; inner diameter of 52 mm, 56 mm, 60 mm, 64 mm, and 68 mm, height of 25 mm, 26 mm, 27 mm, 28 mm, 29 mm, wall thickness of 3 mm, 4 mm, 5 mm, 6 mm, and 7 mm.

The effects of silicone oil on the static stiffness of the damper under the varying structural parameters are shown in Figure 8. When the structural parameters are fixed, the static stiffness of the rubber-silicone oil combined damper is slightly larger compared to the hollow rubber damper. The stiffness of the rubber-silicone oil combined damper is about 0.76% greater than that of the hollow rubber damper. Under varying structural parameters, the effect of silicone oil on the static stiffness of the damper does not follow any obvious trend. The static stiffness decreases with the increase of outer diameter for both the hollow rubber damper and rubber-silicone oil combined damper. However, the static stiffness increases as the inner diameter and wall thickness increase. The static stiffness was found to be consistent as the height were varied.

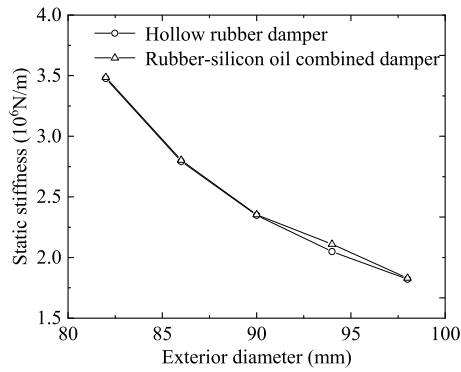
2) EFFECT OF SILICONE OIL VISCOSITY ON STATIC STIFFNESS OF THE DAMPER

To study the effect of silicone oil viscosity on the static stiffness of the rubber-silicone oil combined damper, four types of silicone oil with different viscosities were selected (Table 3) and the effects of oil viscosity on the static stiffness of the damper were analyzed. For ease of description and drawing, the viscosity equal to 0 shown in Figure 8 refers to the viscosity of the hollow rubber damper. The effects of different silicone oil viscosities on static stiffness are shown in Figure 9. As the viscosity of silicone oil increases from 0.096 kg/(m·s) to 12.175 kg/(m·s), the static stiffness of the damper increases by 2.5%.

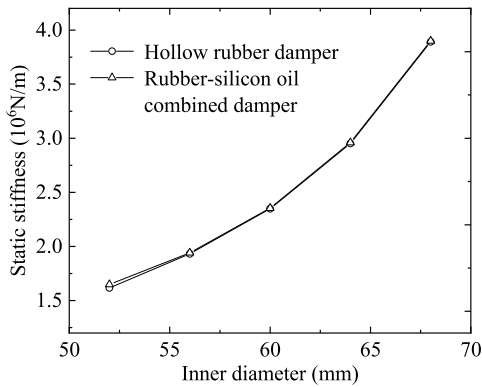
IV. EFFECTS OF SILICONE OIL ON DYNAMIC STIFFNESS AND DAMPING OF RUBBER-SILICONE OIL COMBINED DAMPER

A. SIMULATION AND EXPERIMENTAL VERIFICATION OF DYNAMIC STIFFNESS AND DAMPING CHARACTERISTICS OF COMBINED DAMPER

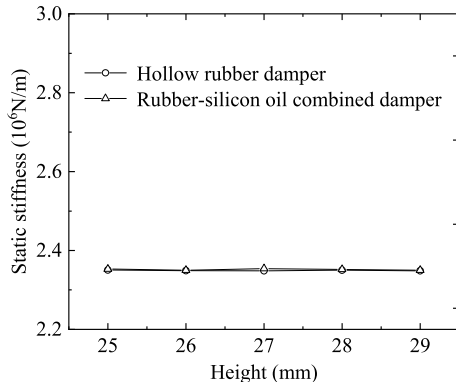
Under dynamic loading, polyurethane rubber is a typical viscoelastic material with a certain correlation between frequency and amplitude. In [21], a medium loss factor $\eta = \tan \delta$ was used to characterize the damping capacity of rubber materials and the loss factor was found to be numerically equal to twice the damping ratio; thus, the damping



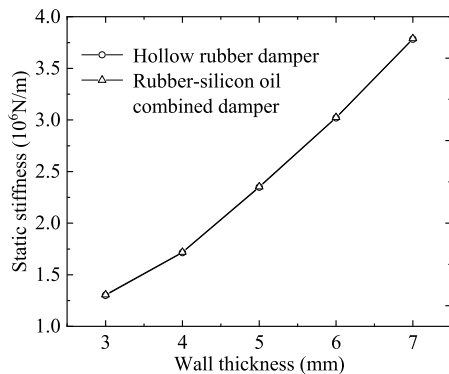
(a) Effect of outer diameter on static stiffness of rubber damper



(b) Effect of inner diameter on static stiffness of rubber damper



(c) Effect of height on static stiffness of rubber damper



(d) Effect of wall thickness on static stiffness of rubber damper

FIGURE 8. Static stiffness of rubber damper in the presence or absence of silicone oil.

characteristics of the damper are reflected by the loss factor. Dynamic stiffness indicates the ability of a material to

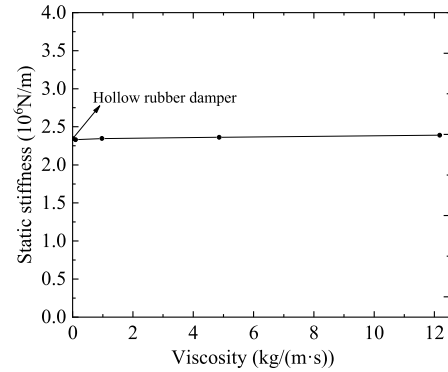


FIGURE 9. Effect of silicone oil viscosity on static stiffness of rubber-silicone oil combined damper.

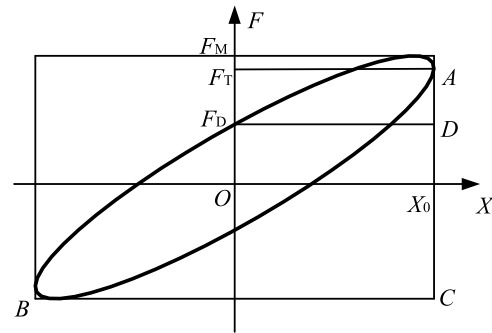


FIGURE 10. Force and deformation hysteresis loop.

resist dynamic deformation, expressed as the dynamic force required to cause one unit of dynamic deformation. This feature can also be used to measure the ability of a structure to resist external dynamic loads and to characterize vibration reduction performance of rubber and other elastomer damping elements [22].

In the present study, the ellipse method was used to solve the dynamic stiffness and loss factor [20]. When a viscoelastic damping system is subjected to harmonic loading, the damping force will be orthogonal to the elastic force and the transmission force will depend on the damping force and elastic force principles. The dynamic stiffness and loss factor can be directly obtained from the transmission force-deformation hysteresis loop (Figure 10): When the displacement reaches the maximum value X_0 , the corresponding transmission force is equal to the elastic force; When the displacement is zero, the damping force reaches the maximum value F_D , and at this time the corresponding transmission force is equal to the damping force.

From Figure 10, the dynamic stiffness can be calculated as

$$K_d = \frac{F_T}{X_0} = \frac{AC}{BC} \quad (5)$$

where AC is twice the elastic force, N; BC is twice the maximum displacement, m; X_0 is the maximum deformation, m; F_M is the transfer force corresponding to the maximum deformation, N, F_T is the maximum elastic force, N.

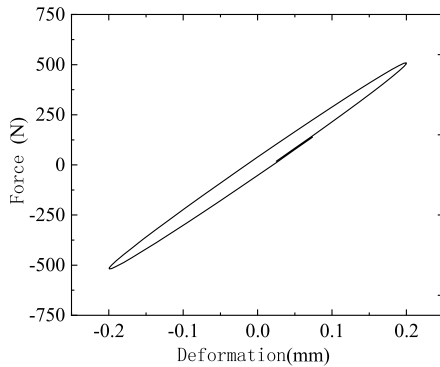


FIGURE 11. Simulation results of dynamic loading of rubber-silicone oil combined damper.

TABLE 4. Comparison of simulation and test results of dynamic loading of rubber-silicone oil combined damper.

Category	Dynamic stiffness	Loss factor
Dynamic simulation	$2.5235 \times 10^6 \text{ N/m}$	0.0783
Dynamic experiment	$2.590 \times 10^6 \text{ N/m}$	0.1250
Error	2.57%	3.74%

The loss factor can be calculated as

$$\eta = \frac{F_D}{F_T} \tag{6}$$

where F_D is the maximum damping force, N.

To study the dynamic stiffness and damping characteristics of the rubber-silicone oil combined damper, the damper was dynamically simulated using an external loading frequency of 1 Hz and amplitude of 0.2 mm. The simulated load-deformation curves are shown in Figure 11. According to equations (5) and (6), the dynamic stiffness is $2.5235 \times 10^6 \text{ N/m}$ and the loss factor is 0.0783.

To verify the dynamic simulation of the rubber-silicone oil combined damper, dynamic tests were carried out on a real rubber-silicone oil combined damper using the same clamping method used in the static tests. For dynamic tests, a radial sinusoidal load was applied. The load-deformation curves obtained using an excitation frequency of 1 Hz and amplitude of 0.2 mm are shown in Figure 12. According to equations (5) and (6), the dynamic stiffness is $2.59 \times 10^6 \text{ N/m}$, and the loss factor is 0.1235. Errors in dynamic stiffness and loss factor between the simulation and test results are presented in Table 4. The dynamic stiffness error is 2.57% and the loss factor error is 3.74%. The errors may be caused by the rubber aging phenomenon, which can occur during storage of the rubber-silicone oil combined damper, and larger stiffness of the clamp compared to the rubber-silicone oil combined damper. Taking these factors into consideration, the results of the simulation are credible and the simulation model is appropriate.

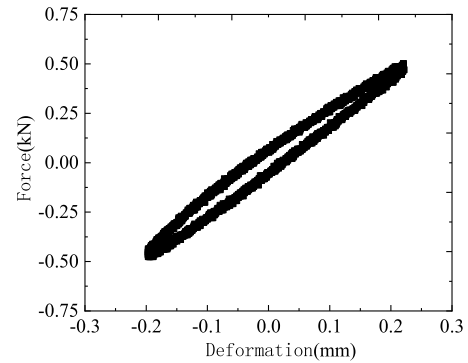


FIGURE 12. Test results of dynamic loading of rubber-silicone oil combined damper.

B. ANALYSIS OF THE EFFECTS OF SILICONE OIL ON DYNAMIC STIFFNESS AND DAMPING OF COMBINED DAMPER

1) THE DYNAMIC STIFFNESS AND DAMPING CHARACTERISTICS OF DAMPER IN THE PRESENCE OR ABSENCE OF SILICONE OIL UNDER DIFFERENT STRUCTURAL PARAMETERS

Under different structural parameters, the presence or absence of silicone oil may have a certain influence on the dynamic stiffness and damping characteristics of the damper. The influence of outer diameter, inner diameter, height, and wall thickness on the dynamic stiffness and damping characteristics of the hollow rubber damper and rubber-silicone oil combined damper were investigated. Furthermore, the influence of the presence or absence effect of silicone oil on the dynamic stiffness and damping characteristics of the damper under different structural parameters were studied. As demonstrated in Section 4.1, the deformation and load generated by the damper under external sinusoidal excitation will form a hysteresis loop, wherein the slope represents dynamic stiffness and the area of the hysteresis loop represents the magnitude of damping. When the outer diameter of the damper changes, the hysteresis loop formed by the damper under an external excitation of 2 Hz and 0.4 mm is shown in Figure 13. With the same outer diameter, the dynamic stiffness of the rubber-silicone oil combined damper and the hollow rubber damper are not significantly different. As the outer diameter increases, the dynamic stiffness gradually decreases.

The effects of the presence or absence of silicone oil on the dynamic stiffness and loss factor of the damper under different structural parameters are shown in Figure 14. The presence or absence of silicone oil has no significant influence on the dynamic stiffness and loss factor of the damper. The dynamic stiffness of the rubber-silicone oil combined damper is slightly higher than that of the hollow rubber damper for the same structural parameters, and the loss factor of the rubber-silicone oil combined damper is also larger; that is, the presence of silicone oil increases the loss factor of the damper by about 10%. The silicone oil

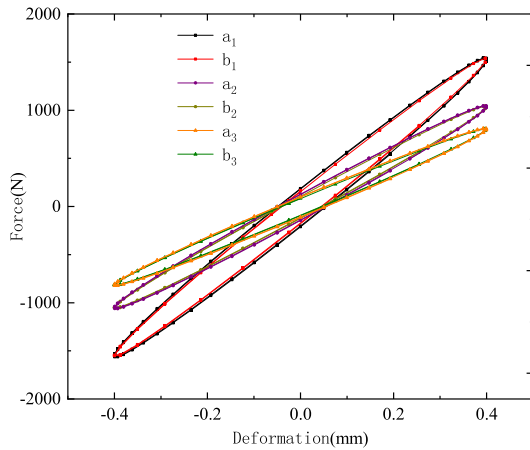
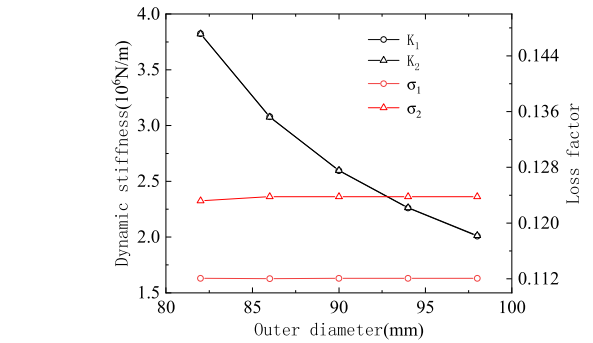


FIGURE 13. Load-deformation curves of damper with or without silicone oil with different damper outer diameter (a1: Rubber-silicone oil combined damper with outer diameter of 82 mm, a2: Rubber-silicone oil combined damper with outer diameter of 90 mm, a3: Rubber-silicone oil combined damper with outer diameter of 98 mm, b1: Hollow rubber damper with outer diameter of 82 mm, b2: Hollow rubber damper with outer diameter of 90 mm, b3: Hollow rubber damper with outer diameter of 98 mm).

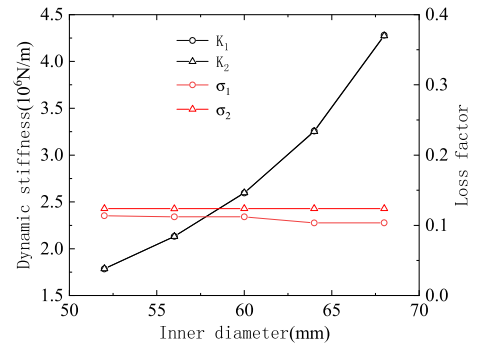
mainly affects the loss factor of the damper, i.e., the damping characteristics.

2) ANALYSIS OF THE PRESENCE OR ABSENCE EFFECT OF SILICONE OIL ON DYNAMIC STIFFNESS AND DAMPING OF DAMPER UNDER DIFFERENT OPERATING CONDITIONS

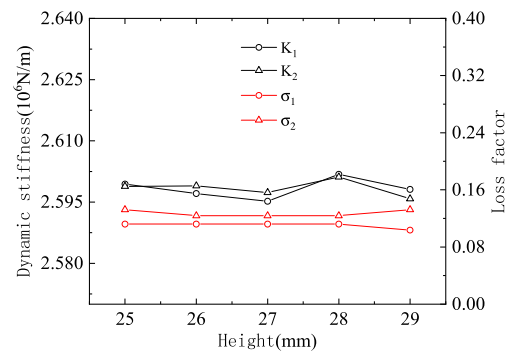
Simulations of the dynamic characteristics of the damper with constant dimensions were carried out at an amplitude of 0.4 mm and external excitation frequencies of 1 Hz, 2 Hz, 3 Hz, 4 Hz, 5 Hz, 6 Hz, 7 Hz, 8 Hz, 10 Hz, 13 Hz and 16 Hz. The viscosity of the silicone oil was 12.175 kg/(m·s) and all other settings were constant (reference values). The simulation results are presented in Figure 15. When the amplitude is constant, the dynamic stiffness of the rubber-silicone oil combined damper increases with increasing external excitation frequency, and the magnitude of this increase gradually decreases. At the same frequency, the dynamic stiffness of the rubber-silicone oil combined damper is slightly larger than that of the hollow rubber damper. As the frequency increases, the presence of silicone oil enhances the difference in dynamic stiffness between the combined and hollow damper. Figure 15(b) shows that the loss factor of the rubber-silicone oil combined damper increases as the external excitation frequency increases, however, the rate of increase gradually decreases. At the same frequency, the loss factor of the rubber-silicone oil combined damper is greater than that of the hollow rubber damper. When the frequency increases from 1 Hz to 16 Hz, the difference in loss factor between the rubber-silicone oil damper and hollow rubber damper also increase. When the frequency is 16 Hz, the loss factor of the rubber-silicone oil damper is about 1.5 times larger compared to the hollow rubber damper. Comparing Figure 15(a) and 15(b), the presence or absence influence of silicone oil on the loss factor of the damper is greater than the influence on dynamic stiffness.



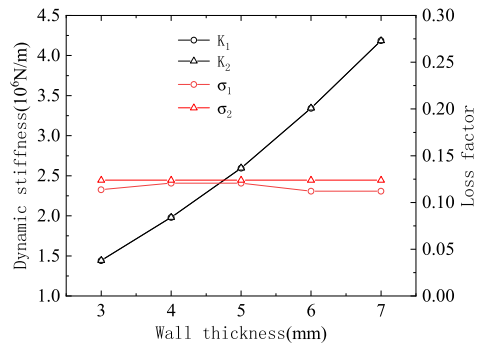
(a) Outer diameter



(b) Inner diameter



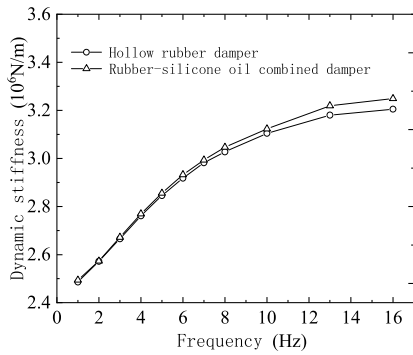
(c) Height



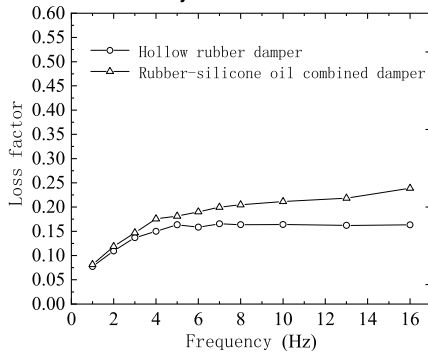
(d) Wall thickness

FIGURE 14. Dynamic stiffness and loss factor of damper in presence or absence of silicone oil with different hollow rubber ring dimensions (k1: Dynamic stiffness of hollow rubber damper, k2: Dynamic stiffness of rubber-silicone oil combined damper, σ_1 : Loss factor of hollow rubber damper, σ_2 : Loss factor of rubber-silicone oil combined damper).

Simulations of the dynamic characteristics of the damper with constant dimensions were carried out at a frequency of 2 Hz and amplitudes of 0.1 mm, 0.2 mm, 0.4 mm,

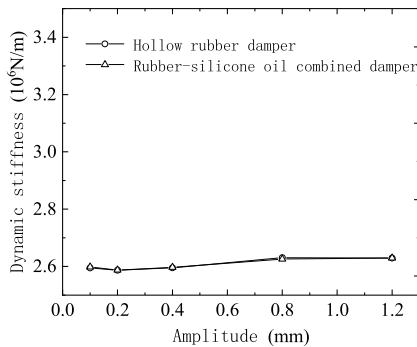


(a) Influence of silicone oil on dynamic stiffness at different frequencies

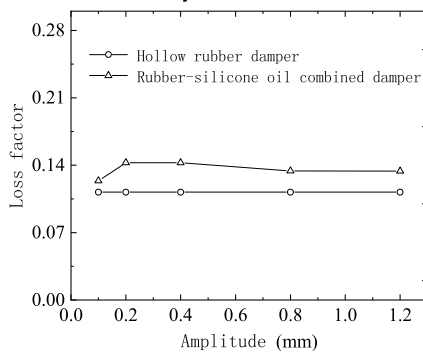


(b) Influence of silicone oil on loss factor at different frequencies

FIGURE 15. Effect of presence or absence of silicone oil on dynamic stiffness and loss factor of the damper at different external excitation frequencies.



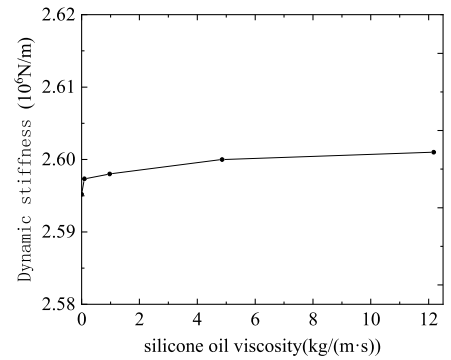
(a) Influence of silicone oil on dynamic stiffness at different amplitudes



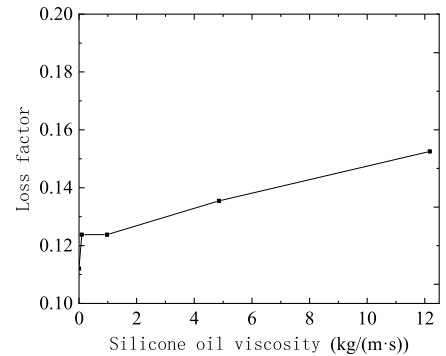
(b) Influence of silicone oil on loss factor at different amplitudes

FIGURE 16. Effect of the presence or absence of silicone oil on the dynamic stiffness and loss factor of the damper at different amplitudes.

0.8 mm, and 1.2 mm. The viscosity of the silicone oil was 12.175 kg/(m·s) and all the other simulation settings were



(a) Influence of silicone oil viscosity on dynamic stiffness



(b) Influence of silicone oil viscosity on loss factor

FIGURE 17. Effects of silicone oil viscosity on dynamic stiffness and loss factor of combined damper.

the same as those described above. The simulation results are presented in Figure 16. Figure 16(a) shows that when the frequency is constant, the dynamic stiffness of the rubber-silicone oil combined damper exhibits an overall increasing trend as the external excitation amplitude increases, however, the increase is only around 1%. At the same amplitude, the gap between the dynamic stiffness of the rubber-silicone oil combined damper and that of the hollow rubber damper is not obvious, indicating that the presence or absence of silicone oil at different excitation amplitudes has very little effect on the dynamic stiffness of the damper. Figure 16(b) shows that the loss factor of the rubber-silicone oil combined damper does not change with changes in the external excitation amplitude. At the same amplitude, the loss factor of the rubber-silicone oil combined damper is greater than that of the hollow rubber damper.

3) ANALYSIS OF THE EFFECT OF SILICONE OIL VISCOSITY ON DYNAMIC STIFFNESS AND DAMPING

To study the effect of silicone oil on the dynamic stiffness and loss factor of the rubber-silicone oil combined damper, silicone oils with four different viscosities were selected, as shown in Table 3. Simulations of the dynamic characteristics of the rubber-silicone oil combined damper were performed. The dimensions of the rubber-silicone oil combined damper remained unchanged and the external excitation was also held constant (2 Hz, 0.4 mm). For ease of description and drawing, the viscosity of 0 refers to the hollow rubber damper. The effect of different silicone oil viscosities on the

dynamic stiffness and damping characteristics are shown in Figure 17.

Figure 17(a) shows that as the viscosity of the silicone oil increases, an overall trend of dynamic stiffness of the rubber-silicone oil combined damper cannot be clearly observed. When the viscosity of the silicone oil in the rubber-silicone oil combined damper increases from 0.096 kg/(m·s) to 12.175 kg/(m·s), the dynamic stiffness of the rubber-silicone oil combined damper changes by only 0.1%. Within the simulation range considered in this paper, silicone oil viscosity was found to have no significant influence on the dynamic stiffness of the damper. From Figure 17(b), it can be seen that as the viscosity of the silicone oil increases, the loss factor of the rubber-silicone oil ring gradually increases. When the viscosity of the silicone oil increases from 0.096 kg/(m·s) to 12.175 kg/(m·s), the loss factor of the rubber-silicone oil combined damper increases by about 10%. Comparing Figure 17(a) and (b), the silicone oil viscosity mainly affects the loss factor, i.e., damping characteristics.

V. CONCLUSION

In this study, static and dynamic simulations of a rubber-silicone oil combined damper were performed in finite element software. Static and dynamic experiments were carried out using a PA-100 electro-hydraulic servo dynamic and static universal testing machine to verify the simulation results. The effects of presence or absence of silicone oil and the viscosity of silicone oil on the static stiffness, dynamic stiffness, and damping characteristics of the damper were analyzed. The main conclusions can be summarized, as follows:

- (1) With different structural parameters, the presence or absence of silicone oil has very little effect on the static stiffness, dynamic stiffness, and loss factor of the damper.
- (2) The dimensions of the hollow rubber damper have the same effect on the static and dynamic stiffness of the damper, which decreases as the outer diameter of the damper increases and increases with increasing inner diameter and wall thickness.
- (3) The loss factor of the damper is not affected by changes in the damper structure. When the dimensions remain constant, there is no obvious difference in stiffness of the rubber-silicone oil combined damper and that of the hollow rubber damper; however, owing to the presence of silicone oil, the loss factor of the rubber-silicone oil combined damper is about 10% higher.
- (4) As the viscosity of the silicone oil increases, the static stiffness, dynamic stiffness, and loss factor of rubber silicone oil dampers increase. Within the scope of this paper, the sensitivity of the three parameters to silicone oil viscosity is loss factor > static stiffness > dynamic stiffness.
- (5) As the external excitation frequency increases, the dynamic stiffness and loss factor of the hollow rubber damper and rubber silicone oil combined

damper increase. The presence of silicone oil increases the difference between the dynamic stiffness and the loss factor.

REFERENCES

- [1] Z. Yanlong, L. Biao, W. Li, and S. Shaoyuan, "Analysis of auto ride comfort based on berg model of rubber bushings," *Noise Vib. Control*, vol. 39, no. 4, pp. 114–119, 2019.
- [2] Y. Zhirong, Q. Chunyun, R. Zhushi, and Z. Qidou, "Design of vibration isolator in ship's thrust bearing," *Noise Vibrat. Control*, vol. 33, no. 06, pp. 211–215, 2013.
- [3] J. Siqin, L. Zhiyuan, L. Feng, and W. Chengpan, "Stiffness analysis and experimental research on rubber of gear box suspender," *Shandong Ind. Technol.*, vol. 19, pp. 215–216, 2017.
- [4] H. Sheng, H. Yifan, W. Xiong, Z. Liji, and Z. Yuqin, "Research progress of rubber and elastomer toughening modified," *China Synth. Resin Plastics*, vol. 36, no. 5, pp. 104–109, 2019.
- [5] W.-S. Lee and S.-K. Youn, "Topology optimization of rubber isolators considering static and dynamic behaviours," *Structural Multidisciplinary Optim.*, vol. 27, no. 4, pp. 284–294, Jun. 2004.
- [6] X. Y. Guo, J. Z. Zhou, D. P. Feng, and H. M. Li, "A method of calculating the dynamic characteristics of rubber isolator," in *Applied Mechanics and Materials*, vol. 395. Zürich, Switzerland: Trans Tech Publ, 2013, pp. 1170–1173.
- [7] L. Yu, S. Liu, L. Ye, G. Huang, and Y. Xu, "The dynamic characteristics of silicone rubber isolator," *J. Wuhan Univ. Technol.-Mater. Sci. Ed.*, vol. 27, no. 1, pp. 130–133, Feb. 2012.
- [8] Z. Youxiang, "The preparation and study of silicone rubber composite dielectric elastomer," M.S. thesis, Mater. Sci. Eng. School, Beijing Univ. Chem. Technol., Beijing, China, 2019.
- [9] Z. Ziqi, M. Ning, W. Qi, N. Chenguang, and D. Xufeng, "Dynamic viscoelastic and nonlinear constitutive model of silicone rubber-based electro-rheological elastomer," *J. Funct. Mater.*, vol. 49, no. 01, pp. 1090–1096, 2018.
- [10] S. W. Wang, Y. Y. Luo, L. Li, and Y. Liu, "Dynamic property analysis of rubber absorber in rail fastenings of different force condition," in *Applied Mechanics and Materials*, vol. 226. Zürich, Switzerland: Trans Tech Publ, 2012, pp. 877–880.
- [11] L. Jingzhi, L. Queyun, and L. Yan, "On dynamic property model of rubber absorber in rail fastening system," *Urban Mass Transit*, vol. 18, no. 12, pp. 84–89, 2015.
- [12] X. Quanshan, Z. Yinglong, and J. Zhu, "On the equivalent test of hyperelastic constitutive model for rubber material of absorber," *Ship Ocean Eng.*, vol. 47, no. 4, pp. 120–124, 2018.
- [13] L. Gang, C. Qian, C. Bao, and Z. Peng, "A study on mechanical behavior of hyperelastic material for rubber bushing," *Mach. Tool Hydraulic Mach. Tool Hydraulic*, vol. 41, no. 18, pp. 19–24, 2013.
- [14] M. A. Abdullah, M. A. Salim, and A. Putra, "Linear and angular displacement relationship of natural rubber engine isolator," in *Applied Mechanics and Materials*, vol. 575. Zürich, Switzerland: Trans Tech Publ, 2014, pp. 250–253.
- [15] M. Liming, Q. Huanyao, Z. Linwei, and L. Houlong, "Application of rubber anti-vibration pad in guideway protective cover for high speed machine," *Coal Mine Machinery*, vol. 39, no. 10, pp. 127–129, 2018.
- [16] L. Keqi, "Dynamic impact simulation and experiment of rubber antivibration system," *J. Railway Sci. Eng.*, vol. 16, no. 1, pp. 192–199, 2019.
- [17] G. Knudsen and J. Keating, "Helicopter drive system on-condition maintenance capability (UH-1/AH-1)," Sikorsky Aircr. Division, United Technol. Corp., Stratford, CT, USA, Tech. Rep., 1976.
- [18] W. Xilong, "Research on the effects of viscoelastic damper to the dynamics of helicopter drive shaft system," M.S. thesis, School Mechtron., Nanjing Univ. Aeronaut. Astronaut., Nanjing, China, 2012.
- [19] W. Weiming, "Study on the stiffness and damping characteristics of annular rubber-silicone oil damper," M.S. thesis, School Mechtron., Nanjing Univ. Aeronaut. Astronaut., Nanjing, China, 2018.
- [20] Standardization Administration, "Vibration and shock isolators measuring method for its static and dynamic characteristics," 2nd ed., Standardization Admin., Beijing, China, Tech. Rep. GB-T/15168 2013, 2013.
- [21] T. Gang, "Preparation and study of damping material based on silicone rubber," M.S. thesis, Mater. Sci. Eng. School, South China Univ. Technol., Guangzhou, China, 2014.
- [22] W. Wenbin, *Mechanical Vibration and Noise*. Beijing, China: Mechanical Industry Press, 2007.



MIAOMIAO LI received the Ph.D. degree in mechanical engineering from the Dalian University of Technology, Dalian, China, in 2012. She is currently with the Nanjing University of Aeronautics and Astronautics. Her main research interest includes vibration of mechanical systems.



WEIFANG CHEN received the Ph.D. degree in mechanical engineering from the Nanjing University of Aeronautics and Astronautics, China, in 2007. Since 1991, she has been with the College of Mechanical and Electrical Engineering, Nanjing University of Aeronautics and Astronautics. Since 2009, she has been a Full Professor. Her research interests include intelligent manufacturing, numerical control machine tool, and motorized spindle design.



JINGYU ZHANG received the master's degree from the Nanjing University of Aeronautics and Astronautics, in 2020. Her main research interest includes mechanical vibration.



CHENG DUAN was a Mechanical Engineer. He is currently with the AECC Hunan Aviation Powerplant Research Institute, Zhuzhou, China.



CHUANGUO WU received the bachelor's degree in mechanical manufacturing and automation from the University of Jinan, Jinan, China, in 2019. He is currently pursuing the master's degree with the Nanjing University of Aeronautics and Astronautics. His main research interest includes vibration of mechanical systems.



RUPENG ZHU received the Ph.D. degree from the Nanjing University of Aeronautics and Astronautics, Nanjing, China, in 2000. He is currently with the Nanjing University of Aeronautics and Astronautics. His main research interest includes mechanical transmission.



XIONG LU was a Mechanical Engineer. He is currently with the AECC Hunan Aviation Powerplant Research Institute, Zhuzhou, China.

...